



Facial Ultrasound Anatomy for Non-invasive Cosmetic and Plastic Surgery Procedures

6

Ximena Wortsman, Camila Ferreira-Wortsman, and Natacha Quezada

Contents

6.1 The Role of Sonography in Cosmetic and Plastic Surgery	147
6.2 Main Anatomical Layers of the Face	148
6.2.1 Muscles of the Face.....	153
6.2.2 Main Vessels of the Face.....	155
6.2.3 Anatomy of the Eyelids and Periorbital Region.....	155
6.3 Sonographic Evaluation of Facial Structures	155
References	178

6.1 The Role of Sonography in Cosmetic and Plastic Surgery

Several anatomical structures of the face may be critical for performing cosmetic or plastic surgery procedures. For example, the injection of Botulinum toxin type A in the wrong place may produce an unwanted effect such as an eyelid ptosis. Another example of an adverse reaction may follow the unintended intravascular injection of fillers in the glabellar or nasofold regions, which can cause skin necrosis and blindness [1]. Fortunately, in spite of the large and rising numbers of cosmetic procedures that are performed worldwide, reports of very severe adverse reactions seem to be infrequent; most adverse reactions are transitory and manageable. However, knowledge of the precise anatomical characteristics and location of these structures may support the prevention and/or early detection of these troublesome and sometimes devastating side effects [2, 3].

Sonography can show the location and thickness of muscles, arteries, veins, and glands, including the presence of anatomical variants. It provides non-invasive imaging of the eyelids, nose, and lips and can detect the presence and location of exogenous material such as fillers [4].

6.2 Main Anatomical Layers of the Face

The face is composed of several layers such as: [1–3]:

1. Skin: Epidermis, dermis, and hypodermis (also called subcutaneous tissue), including superficial fat pads
2. Superficial muscular-aponeurotic system (SMAS), defined as a network of connective tissue with fibrous and elastic components, which is located between the skin and the muscles

3. Muscles

4. Bones

Between these layers, there are deep fat pads, arteries, veins, nerves, glands, and cartilages. Figures 6.1, 6.2, 6.3, 6.4, 6.5, 6.6, 6.7, 6.8, 6.9, and 6.10 illustrate and describe the relevant facial anatomical structures. Moreover, the aging process produces changes in the anatomical layers of the face that are evidenced by common lines and wrinkles (Fig. 6.11).

Fig. 6.1 Superficial fat pads of the face (front view).

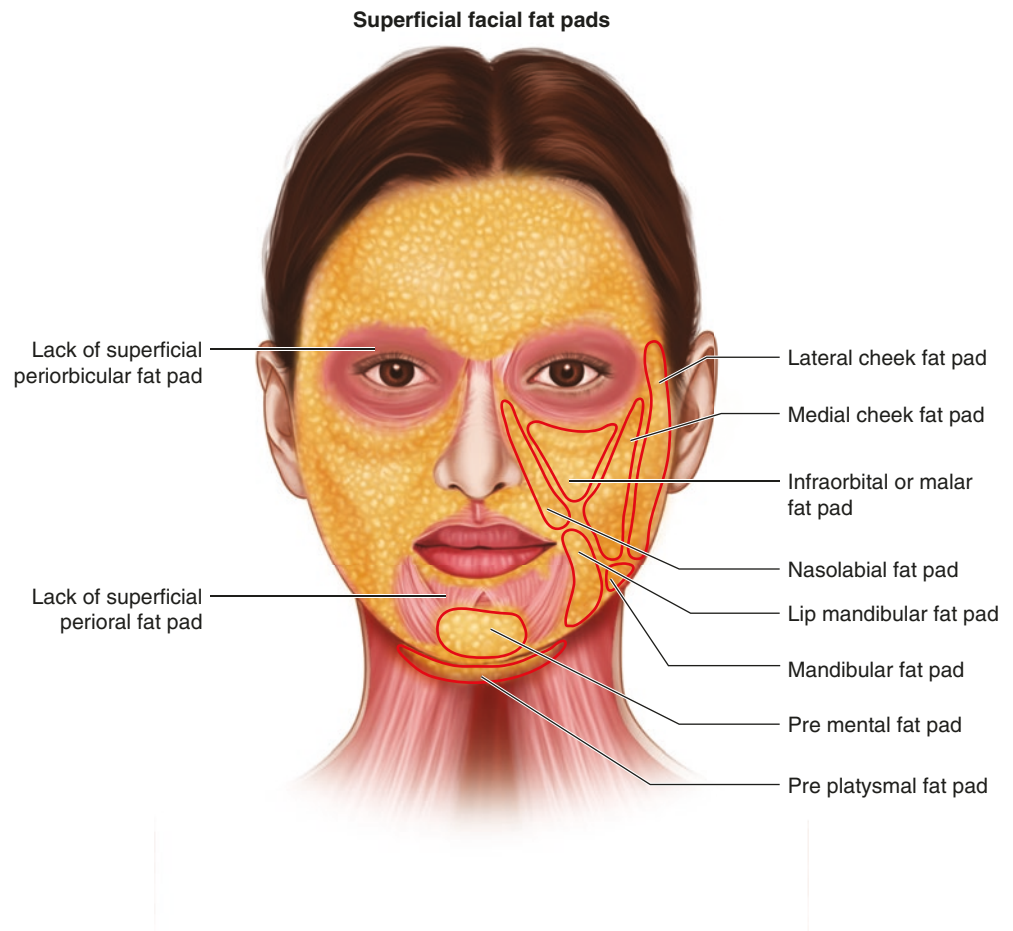
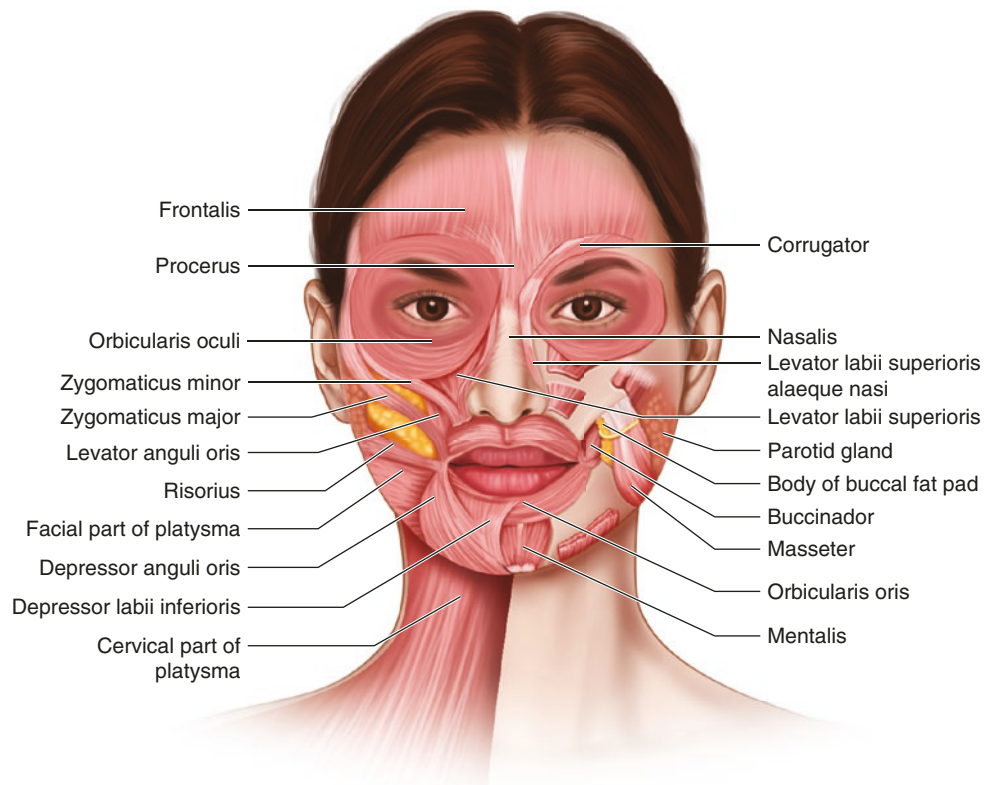


Fig. 6.2 Muscles of the face (front view).



Deep Facial Fat Pads

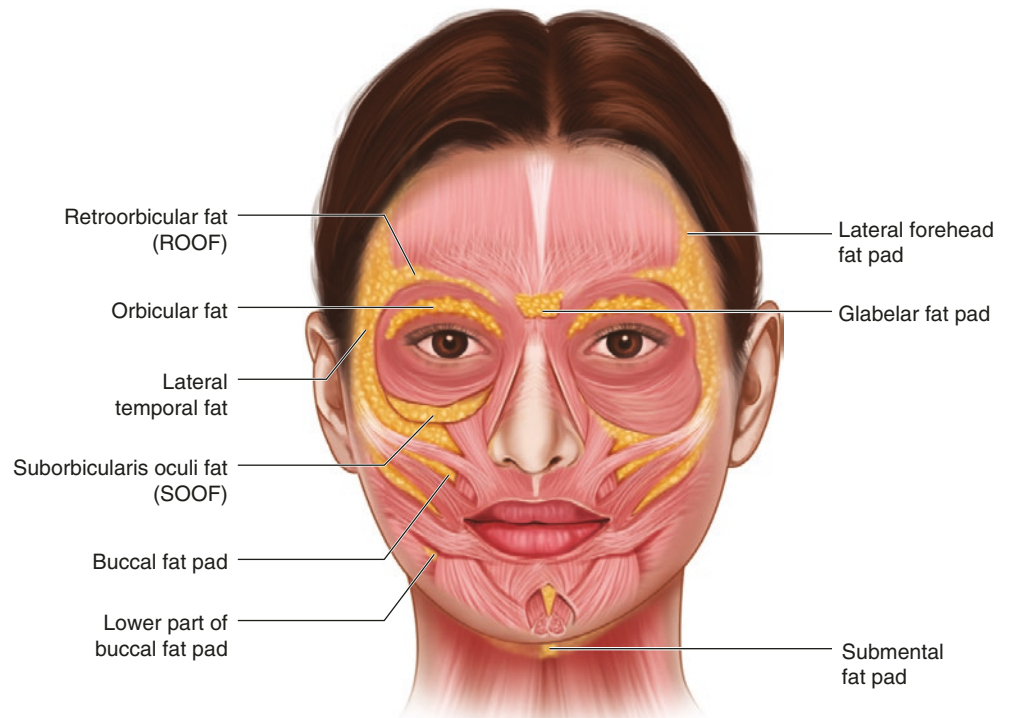


Fig. 6.3 Deep fat pads of the face (front view). ROOF—retro-orbicularis oculi fat; SOOF—suborbicularis oculi fat.

Fig. 6.4 Vessels of the face (front view).

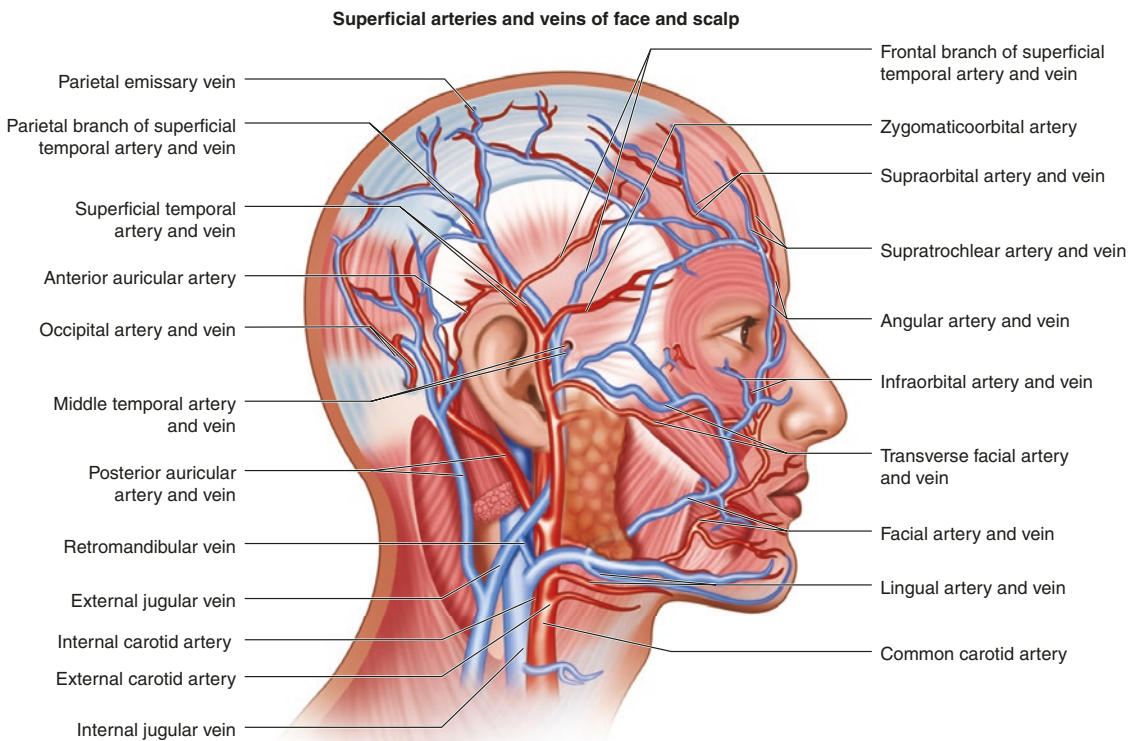
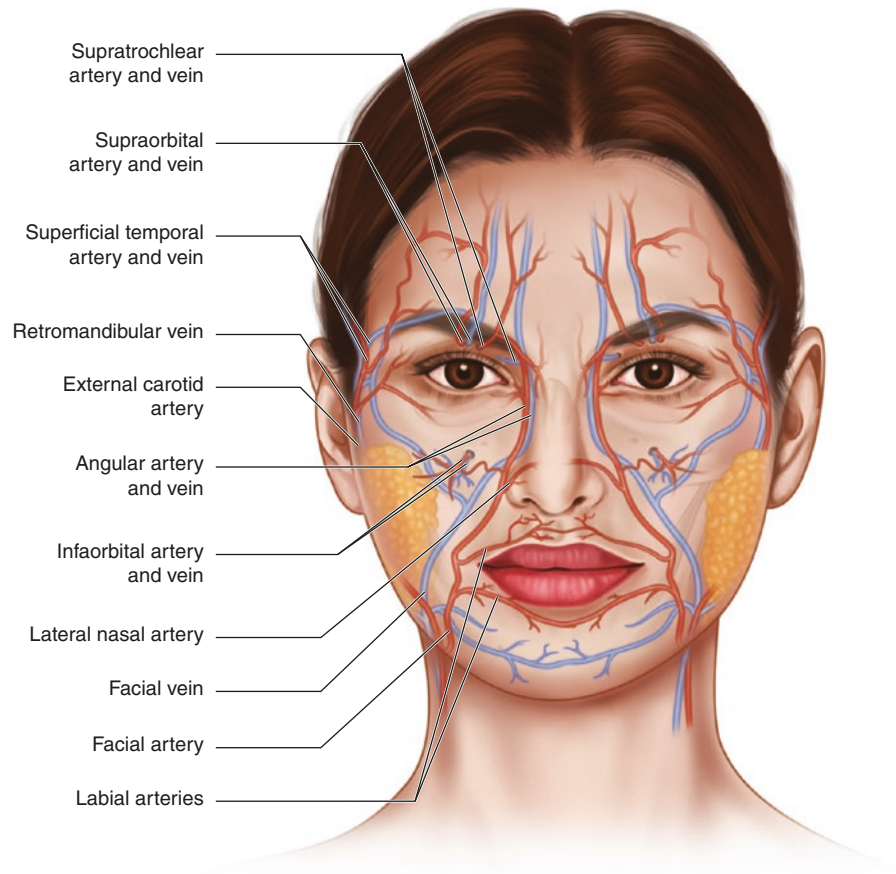


Fig. 6.5 Vessels of the face and scalp (lateral view).

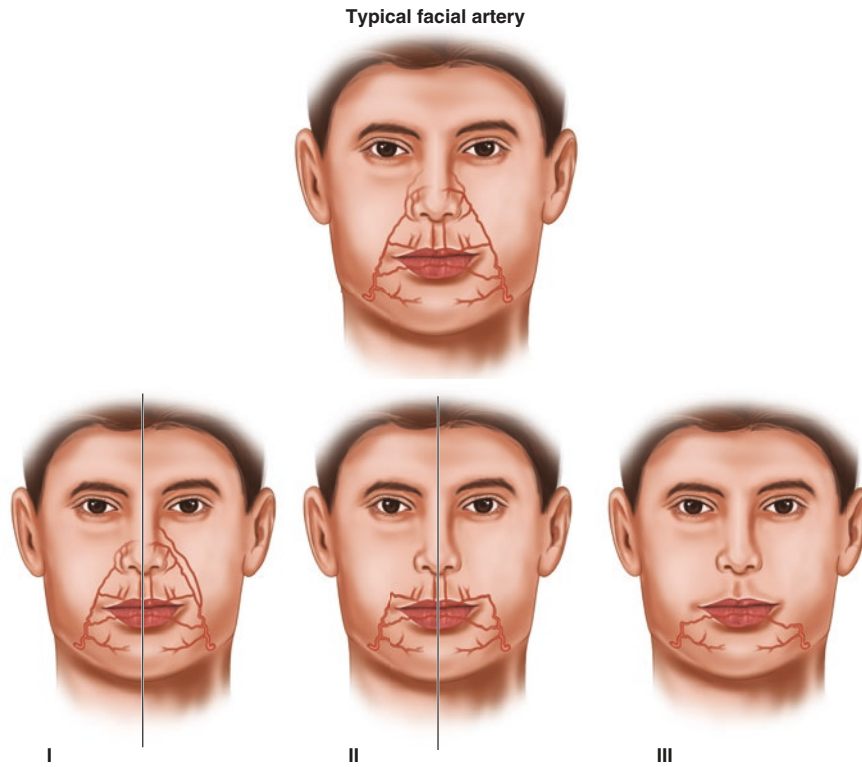


Fig. 6.6 Classic path of the facial artery and its angular and labial branches (top), and some anatomical variants (I–III).

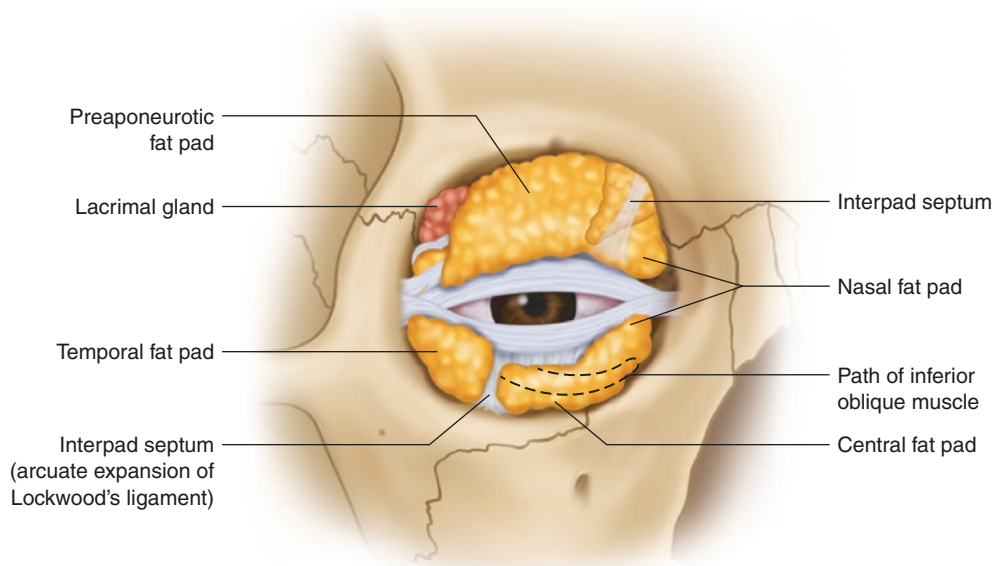


Fig. 6.7 Orbital fat pads and related structures.

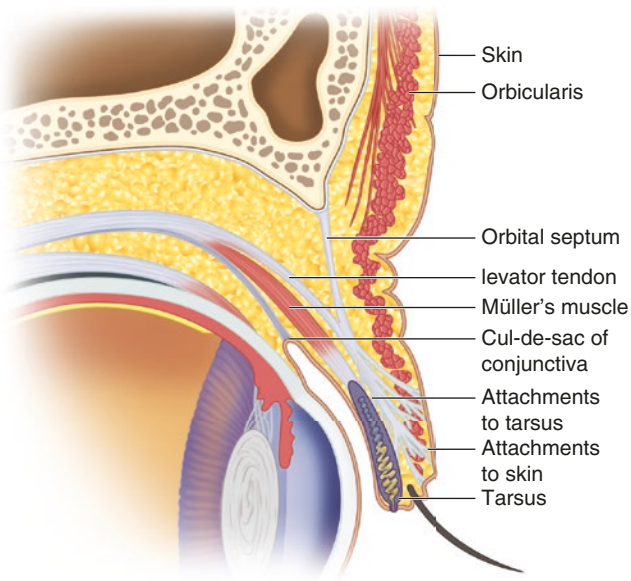


Fig. 6.8 Upper eyelid (lateral view).

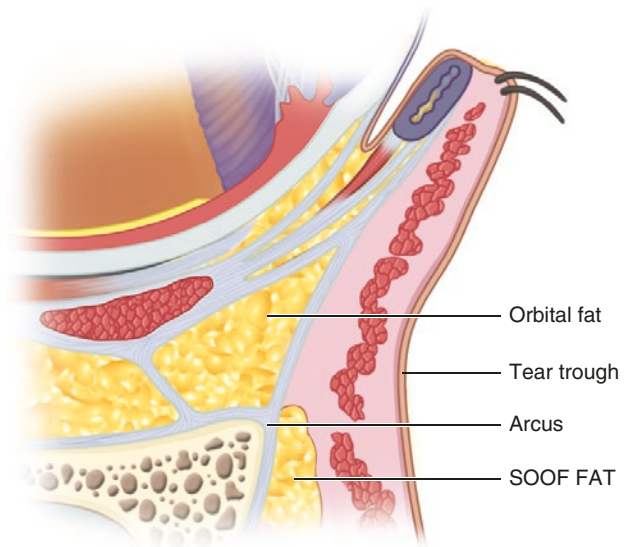


Fig. 6.9 Lower eyelid (lateral view). SOOF—suborbicularis oculi fat.

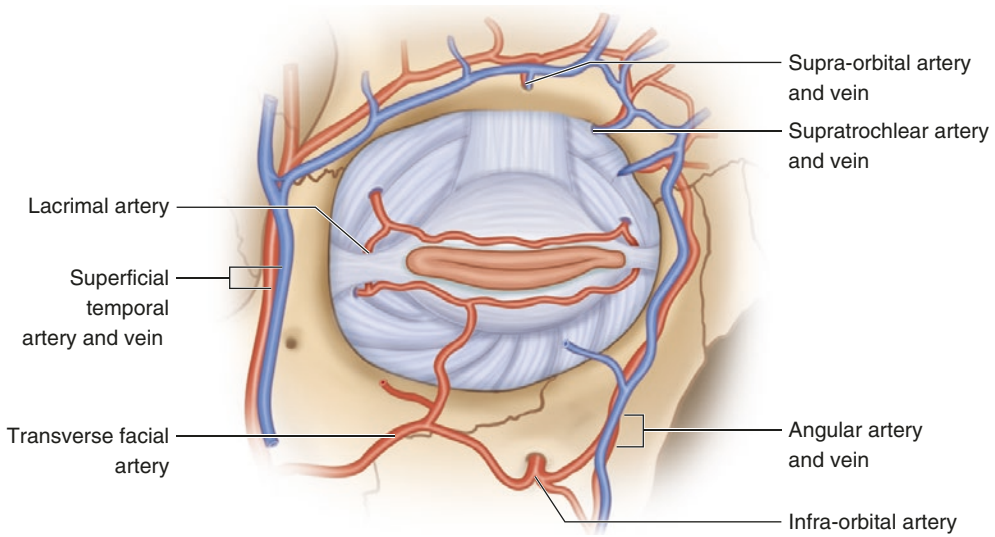


Fig. 6.10 Vessels of the orbit. The lateral aspect is located on the left and medial aspect on the right of the drawing.

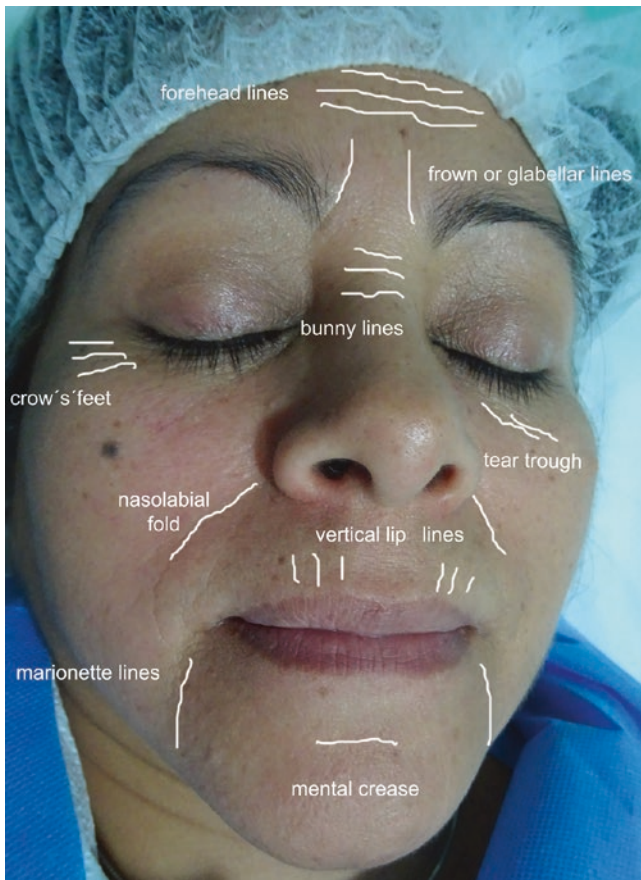


Fig. 6.11 Frequent facial wrinkles and lines.

6.2.1 Muscles of the Face

Most cosmetic procedures deal with the so-called facial expression muscles [5–8]. These include several muscles around the main cavities of the face, such as the orbit and the mouth. Interestingly, some of these muscles, such as the zygomaticus or risorius muscles, are very thin and may show prominent fibrous parts. Other muscles, such as the orbicularis oculi, present loose insertions into the fibrofatty hypodermal tissue, or they can end in a common muscular site such as the modiolus region of intersection of the peribuccal muscles. These muscles support the expression of emotions by playing agonist-antagonist roles and are mostly innervated by branches of the facial nerve. Cosmetic procedures such as botulinum toxin injections are intended to decrease the strength of the muscles that generate unwanted lines or wrinkles by a powerful contraction.

An illustration of the muscles of the face is shown in Fig. 6.2. Table 6.1 summarizes the origin, insertion, and action of facial muscles, and the wrinkles derived from their actions [9–18].

Table 6.1 Muscles of the face

Muscle name	Origin	Insertion	Actions	Comments	Wrinkles
Frontalis or Epicranius	Galea aponeurotica	Orbicularis Oculi muscle, Procerus muscle, Hypodermis of the eyebrows	Raise eyebrows	No bony attachment 88% individuals show bifurcation 46% of these 88% show microscopic muscle fibers at the bifurcation and beyond	Horizontal forehead lines
Corrugator	Medial supraorbital rim 46% Medial frontal bone 31% Medial infraorbital rim 17% Upper nasal process 7%	Medial half of the hypodermis of the eyebrows	Frowning angry expressions. Pull medial part of eyebrows together	The superior and lateral fibers are interdigitated with the frontalis muscle	Vertical glabellar or frown lines
Orbicularis Oculi	Frontal bone Maxillary bone	Fibrofatty tissue of the eyelids Palpebral ligaments	Orbital part: close eyelids voluntarily Palpebral part: close eyelids involuntarily (blinking reflex) Lacrimal part: compresses the lacrimal sac and supports the flow of tears	Circle-shaped muscle with 3 parts: Orbital orbicularis: ellipse-shaped, outer and outer part Palpebral orbicularis: located in the upper and lower eyelids Lacrimal orbicularis or tensor tarsi antagonist: levator palpebrae superioris	crow's feet lines tear troughs nasojugal groove
Procerus	Fascia on top of nasal bones	Fibrofatty glabellar tissue and frontal musculoaponeurotic layer	Frowning downward Very angry expressions	Pull the medial part of eyebrows downward Flaring nostrils It has a triangular shape	Horizontal or bunny lines

(continued)

Table 6.1 (continued)

Muscle name	Origin	Insertion	Actions	Comments	Wrinkles
Zygomaticus Major	Zygomatic bone	Modiolus	Smiling	Raise the angle of the mouth upward and laterally 34% can show a bifid structure lateral to the zygomatic minor muscle	Nasolabial lines Midcheek lines or furrows
Zygomaticus Minor	Zygomatic bone	Fibrofatty hypodermal tissue	Sad facial expressions	Move upper lip backward, upward, and outward It has a fibrous component	Nasolabial lines
Levator Labii Superioris	Medial infraorbital margin	Orbicularis oris Fibrofatty tissue of the upper lip	Elevation of the upper lip	Some fibers merge with the procerus muscle	Vertical lines upper lip Nasolabial lines
Levator Labii Superioris Alaeque Nasi	Nasal and maxillary bones	Lateral fibrofatty tissue of the nostrils, alar cartilages and muscular layer of the upper lip	Dilation of nostrils Elevation of the upper lip Elevation of the wings of the nose	Merge with fibers of the nasalis muscle Due to its action it has been called “Elvis muscle” in remembrance of the expressions commonly performed by the singer Elvis Presley	Nasojugal groove
Levator Anguli Oris	Maxillary bone canine fossa	Modiolus	Smiling Elevation of the upper lip	Also called caninus muscle	
Risorius	Parotid fascia Masseter fascia Platysma	Modiolus	Lateral smiling Pulls backward the angles of the mouth	Thin bundle with prominent fibrous component It may partially cover the masseter muscle	
Orbicularis Oris	Maxilla Mandible	Fibrofatty tissue of the lips	Puckering the lips Kissing	Circle-shaped muscle connected to other muscles in the modiolus region	Vertical upper lip lines
Depressor Anguli Oris	Tubercle of mandible	Modiolus	Lower and lateral displacement of the angles of the mouth Sadness expression	Also called Triangular muscle	Marionette lines
Depressor Labii inferioris	Oblique line of mandible	Fibrofatty tissue of the lower lip	Depression of the lower lip Sadness expression	Also called Quadratus muscle Fibers blend with orbicularis oris muscle	
Mentalis	Anterior mandible	Fibrofatty tissue of the lower lip	Protrusion lower lip Elevation of the soft tissues of the chin Pout expression	Paired muscle	Crease lines at the chin
Masseter	Zygomatic arch Maxillary process of the zygomatic bone	Angle and lateral surface of the ramus of the mandible Coronoid process	Mastication	Elevation of the mandible necessary for closing the mouth hypertrophy affects the lateral shape of the lower face	
Platysma	Fibrofatty tissue of the infraclavicular and acromial regions Fascial layers of the pectoralis and deltoid muscles	Anterior and lateral parts of the mandible Fibrofatty tissue of the chin	Lower the mandible and corners of the mouth Stress or tension expression in the face and neck Sadness expression	Thin band of muscle that overlaps the Sternocleidomastoid Pectoralis major and Deltoid muscles	Marionette lines Medial neck vertical lines Chin crease or dimpling
Nasalis	Medial aspect of the maxilla	Nasal bones	Elevation of the nostrils Depression of the tip of the nose Compression of the bridge of the nose	It has 2 parts Transverse: covers the bridge of the nose Alar: attached to the alar cartilages	

6.2.2 Main Vessels of the Face

The location of some vessels produces danger regions in cosmetic and plastic surgery procedures. Among the most relevant are the facial artery and its branches, such as the angular and labial arteries. Illustrations of the distribution of the main vessels of the face and some anatomical variants of the facial and labial arteries [19–22] are shown in Figs. 6.4, 6.5, and 6.6.

6.2.3 Anatomy of the Eyelids and Periorbital Region

Several cosmetic and plastic surgery procedures are performed around the eyelids and periorbital regions [23, 24], so knowledge of the regional anatomy is of paramount importance. Figs. 6.7, 6.8, 6.9, and 6.10 illustrate the anatomy of these areas.

6.3 Sonographic Evaluation of Facial Structures

The ultrasound evaluation of facial structures can be relevant for the assessment of the regional anatomy, ruling out variants or a dystrophic presence of the components of the layers of the face. Additionally, the effects of facial nerve paralysis have been studied on ultrasound [25–30]. Sonography has proved useful in the evaluation of the masseter muscle in bruxism and its effects on the shape of the lower face [31]. These sonographic data may support more precise planning of the cosmetic or surgical procedures in this region.

Figures 6.12, 6.13, 6.14, 6.15, 6.16, 6.17, 6.18, 6.19, 6.20, 6.21, 6.22, 6.23, 6.24, 6.25, 6.26, 6.27, 6.28, 6.29, and 6.30 show a correlation of clinical and sonographic images. They include the recommended positions of the probe for faster tracking of the structures. Once a structure is detected in the suggested axis, the probe is rotated in order to study the perpendicular axis of the same structure.



Fig. 6.12 Frontalis muscle. (a) Clinical image shows the location of the probe. (b) Ultrasound (transverse axis) demonstrates the hypoechoic structure of the frontalis muscle (asterisks). Notice the thin musculo-aponeurotic layer at the frontal region.

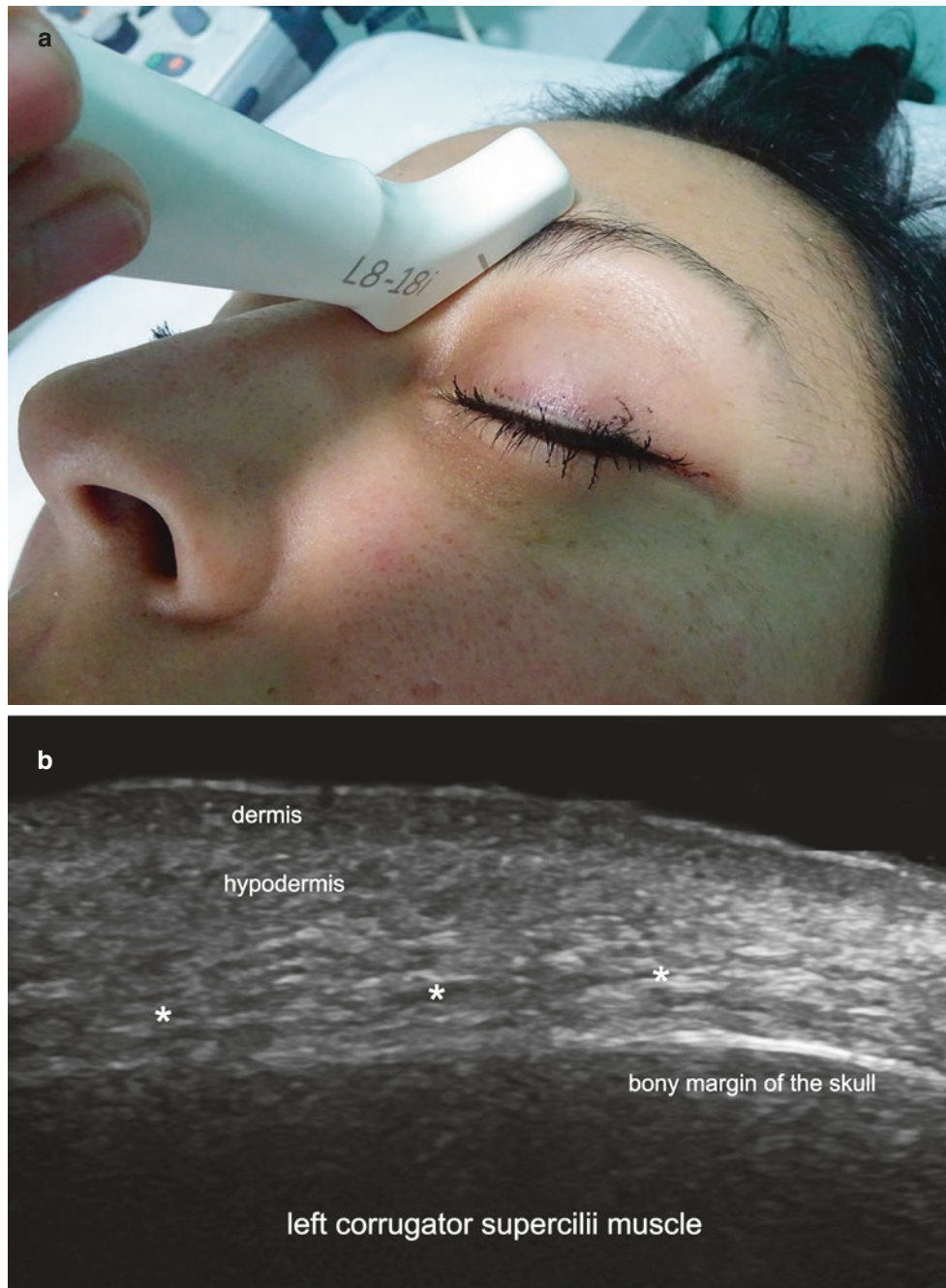
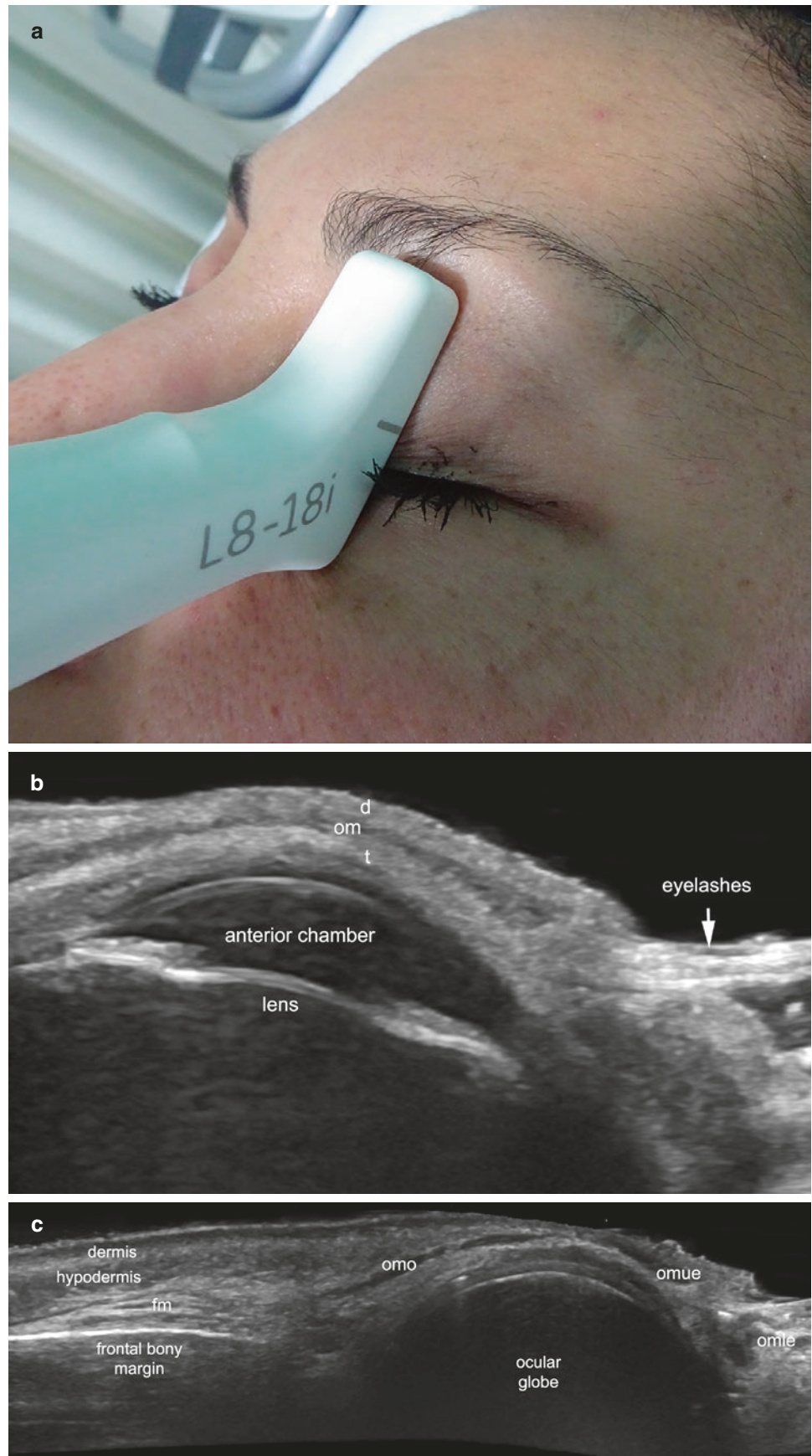


Fig. 6.13 Corrugator muscle. (a) Clinical image shows the location of the probe. (b) Ultrasound (oblique axis) demonstrates the deep location of the corrugator muscle (asterisks).

Fig. 6.14 Orbicularis muscle upper part (orbital and palpebral). (a) Clinical image shows the location of the probe. (b) Ultrasound (longitudinal axis) shows the thin hypoechoic band of the upper palpebral part of the orbicularis muscle (om). (c) Ultrasound panoramic longitudinal view demonstrates the upper orbicularis muscle orbital part (omo) and palpebral part (omue), as well as the lower palpebral part of the orbicularis muscle (omle). *fm* frontalis muscle, *t* tarsal plate.



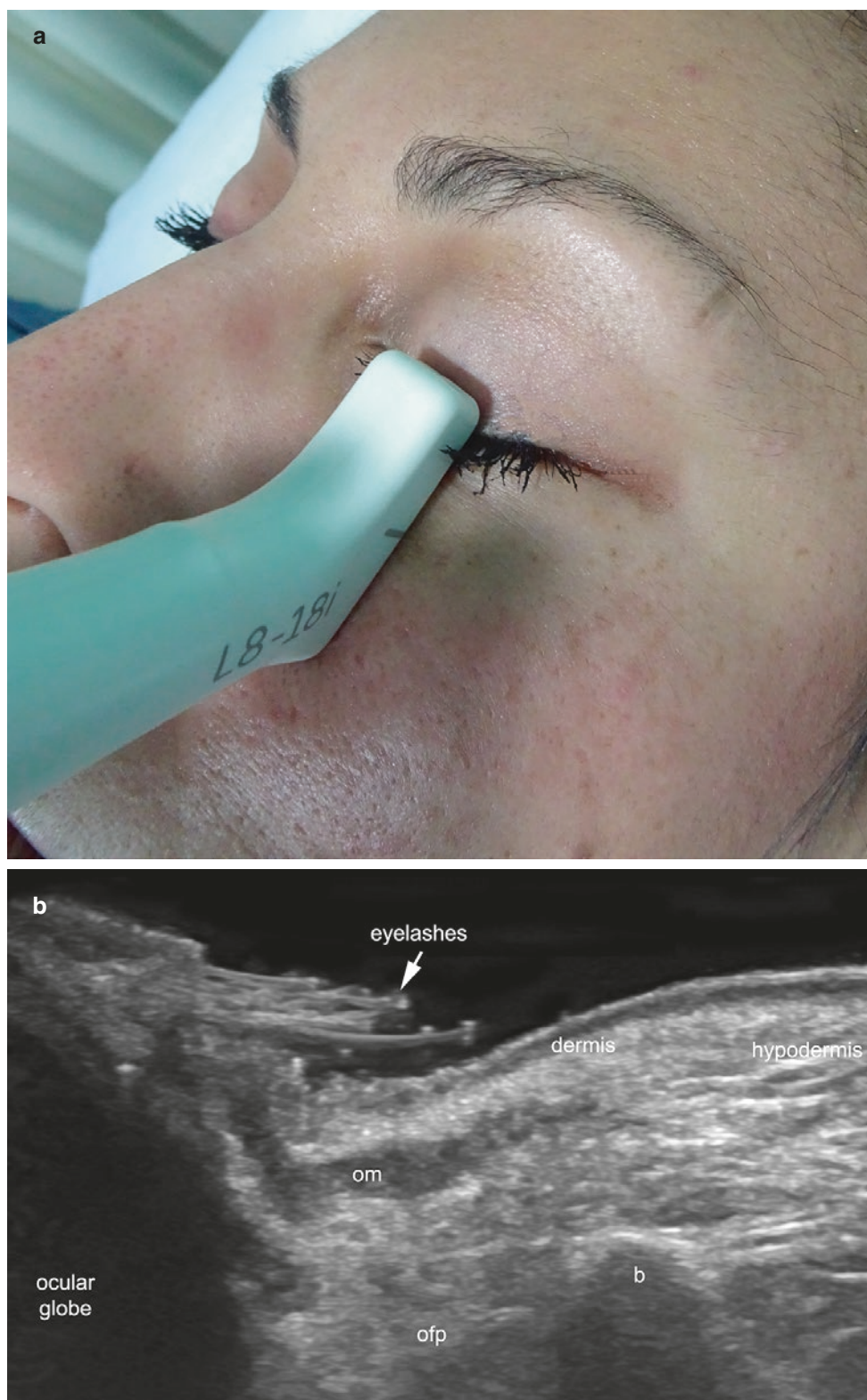


Fig. 6.15 Orbicularis muscle lower part (orbital and palpebral). (a) Clinical image shows the location of the probe. (b) Ultrasound (longitudinal axis) demonstrates the hypoechoic thin band of the palpebral

and orbital part of the orbicularis muscle (om). Notice the distal insertion of the orbicularis muscle in the superficial fibrofatty hypodermal tissue and the eyelashes (*arrow*). *B* bony margin, *ofp* orbital fat pad.

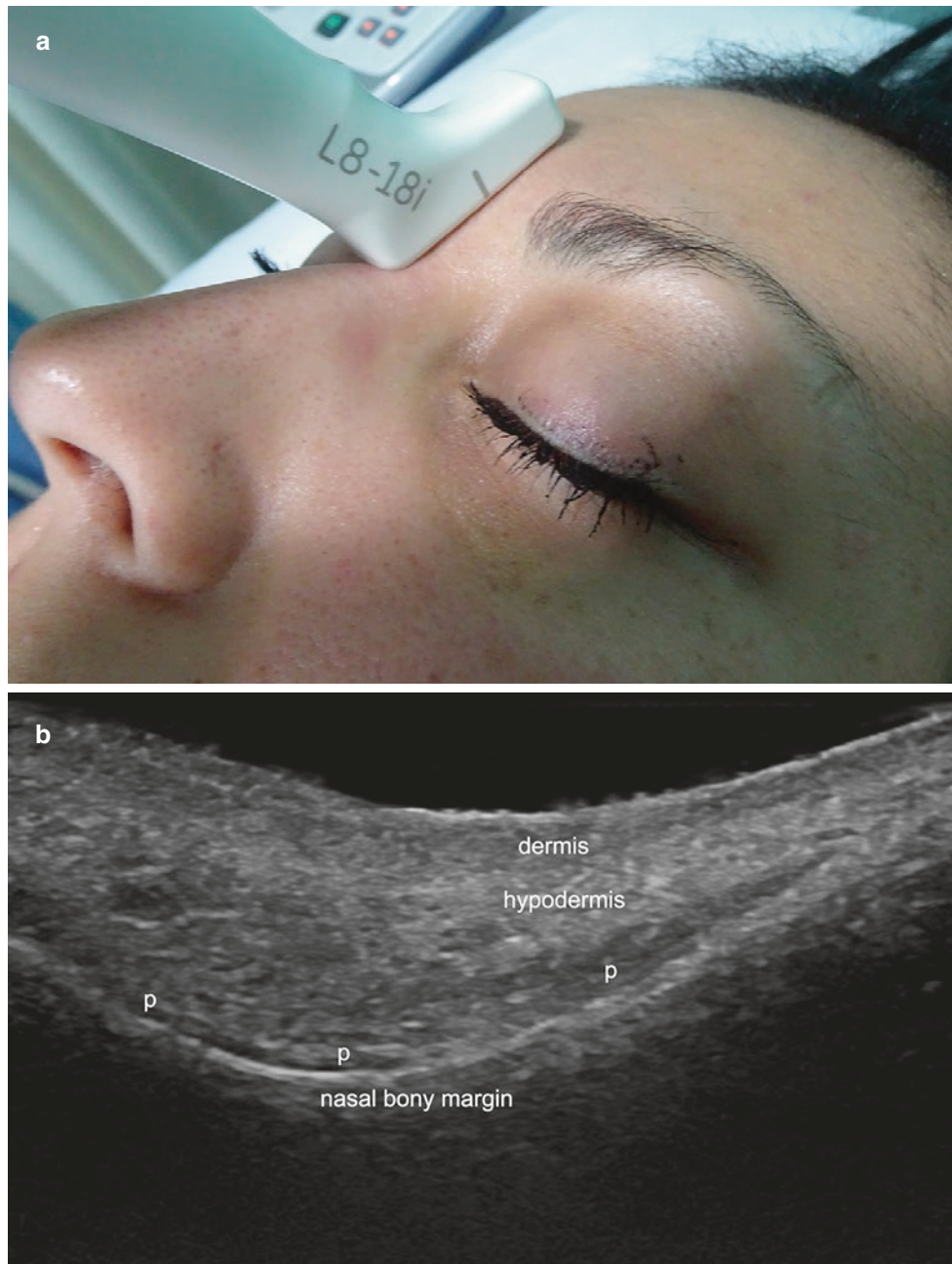
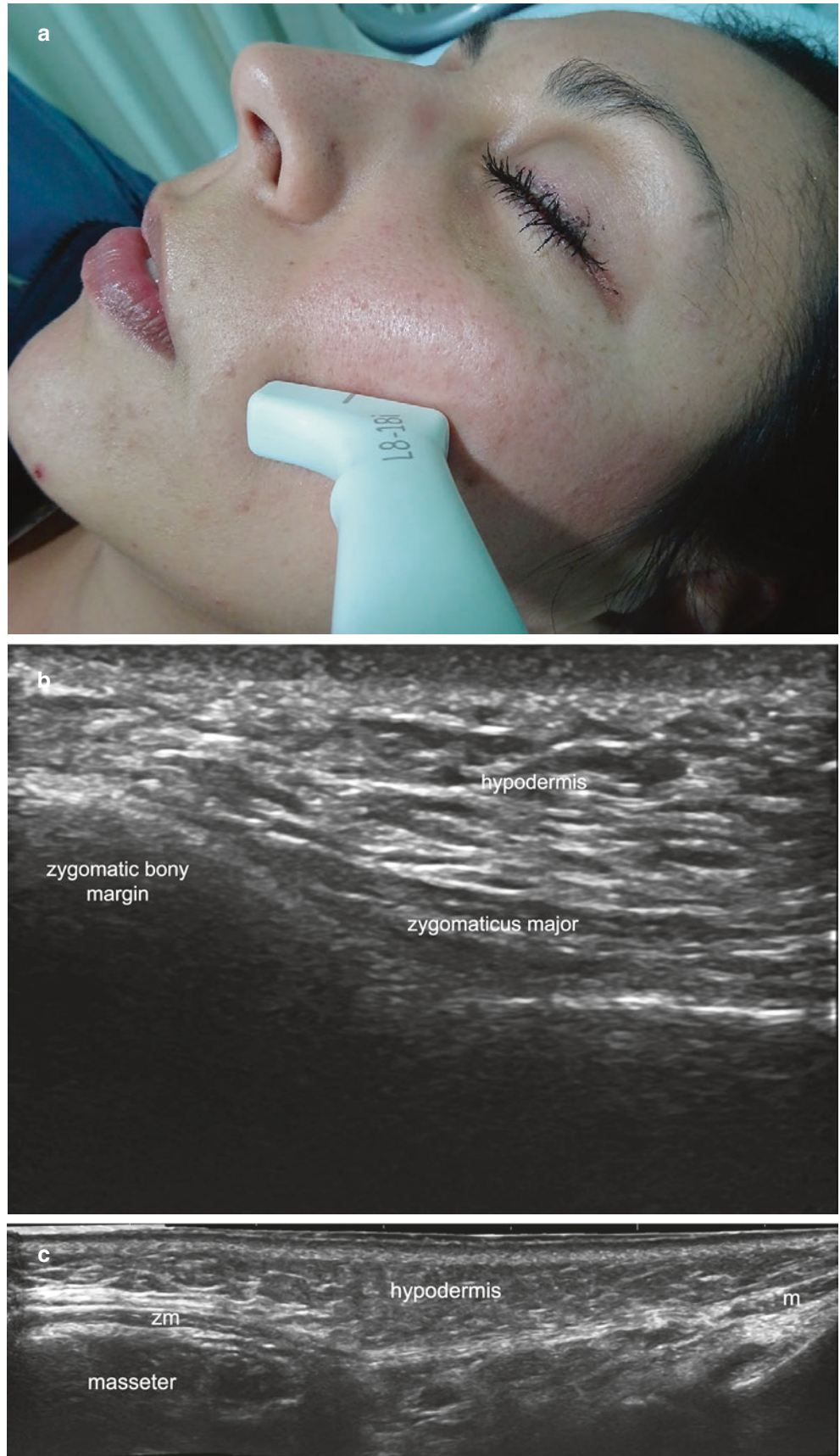


Fig. 6.16 Procerus muscle. (a) Clinical image shows the location of the probe. (b) Ultrasound (longitudinal axis) shows the hypoechoic thin structure of the procerus (p) muscle attached to the bony margin (b) of the nasal bones.

Fig. 6.17 Zygomaticus major muscle. (a) Clinical image shows the location of the probe. (b) Ultrasound (longitudinal oblique axis at the proximal part) and (c) Ultrasound (longitudinal oblique panoramic view) present the hypoechoic thin structure of the zygomaticus muscle (zm) at the proximal part and the thin, hyperechoic band at the distal part close to the distal insertion at the modiolus (m).



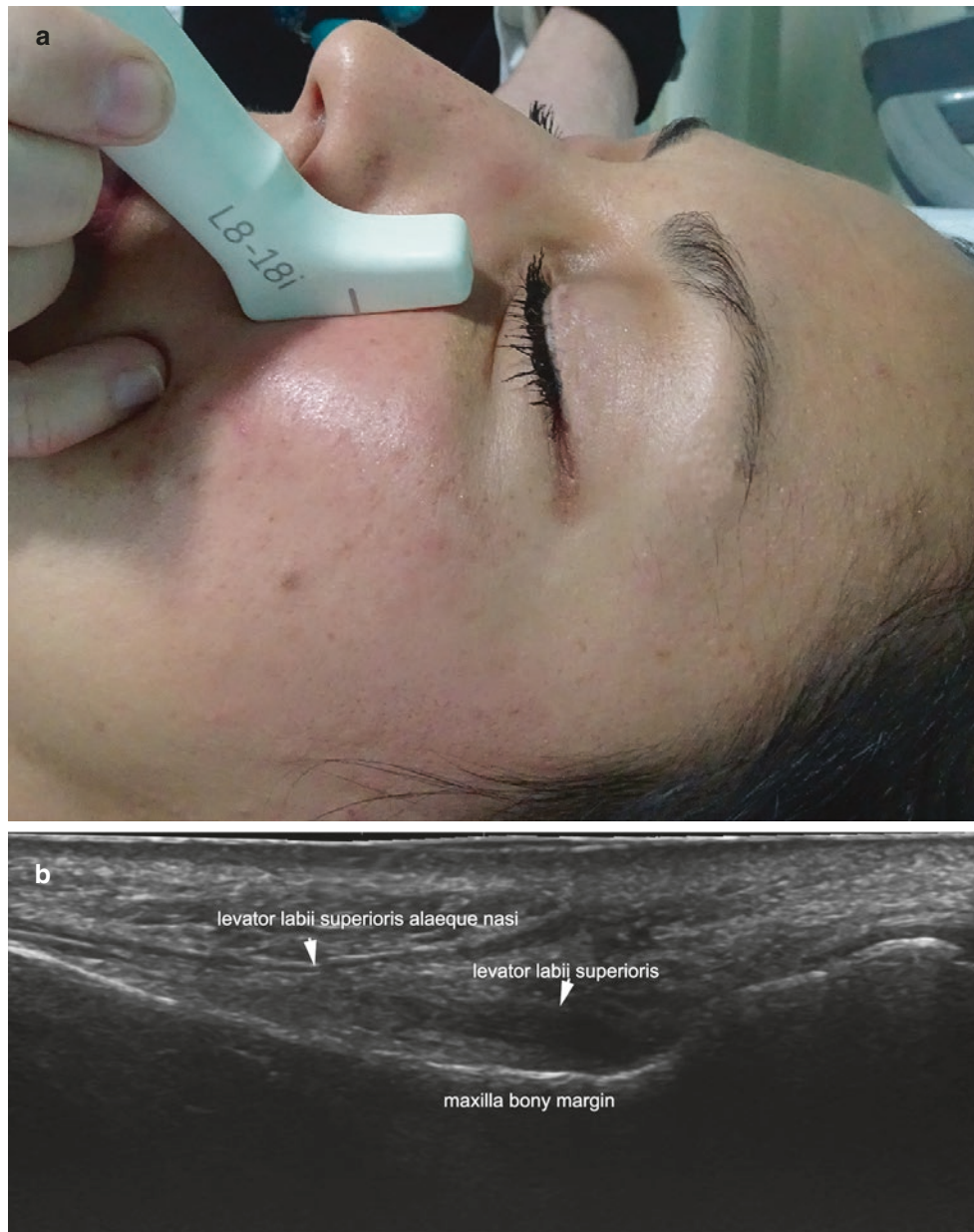


Fig. 6.18 Levator labii superioris and levator labii superioris alaeque nasi muscles. (a) Clinical image shows the location of the probe. (b) Ultrasound (longitudinal axis) demonstrates the hypoechoic band of the

levator labii superioris. Notice that the levator labii superioris muscle is thicker at the distal part (*arrow*) and the close and superficial location of the levator labii superioris alaeque nasi muscle.

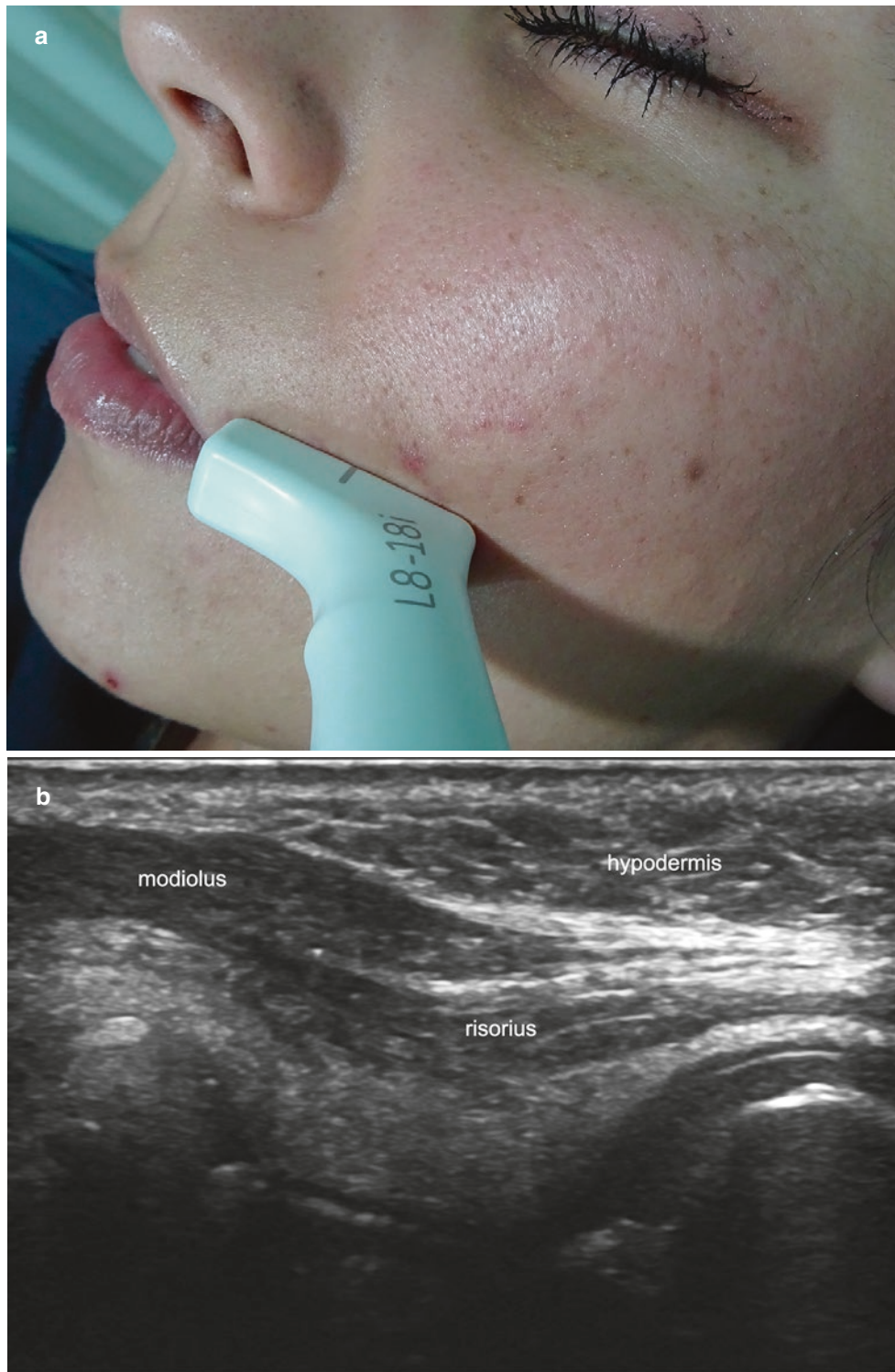


Fig. 6.19 Risorius muscle. (a) Clinical image shows the location of the probe. (b) Ultrasound (longitudinal axis) demonstrates the hypoechoic band of the risorius muscle close to the modiolus.

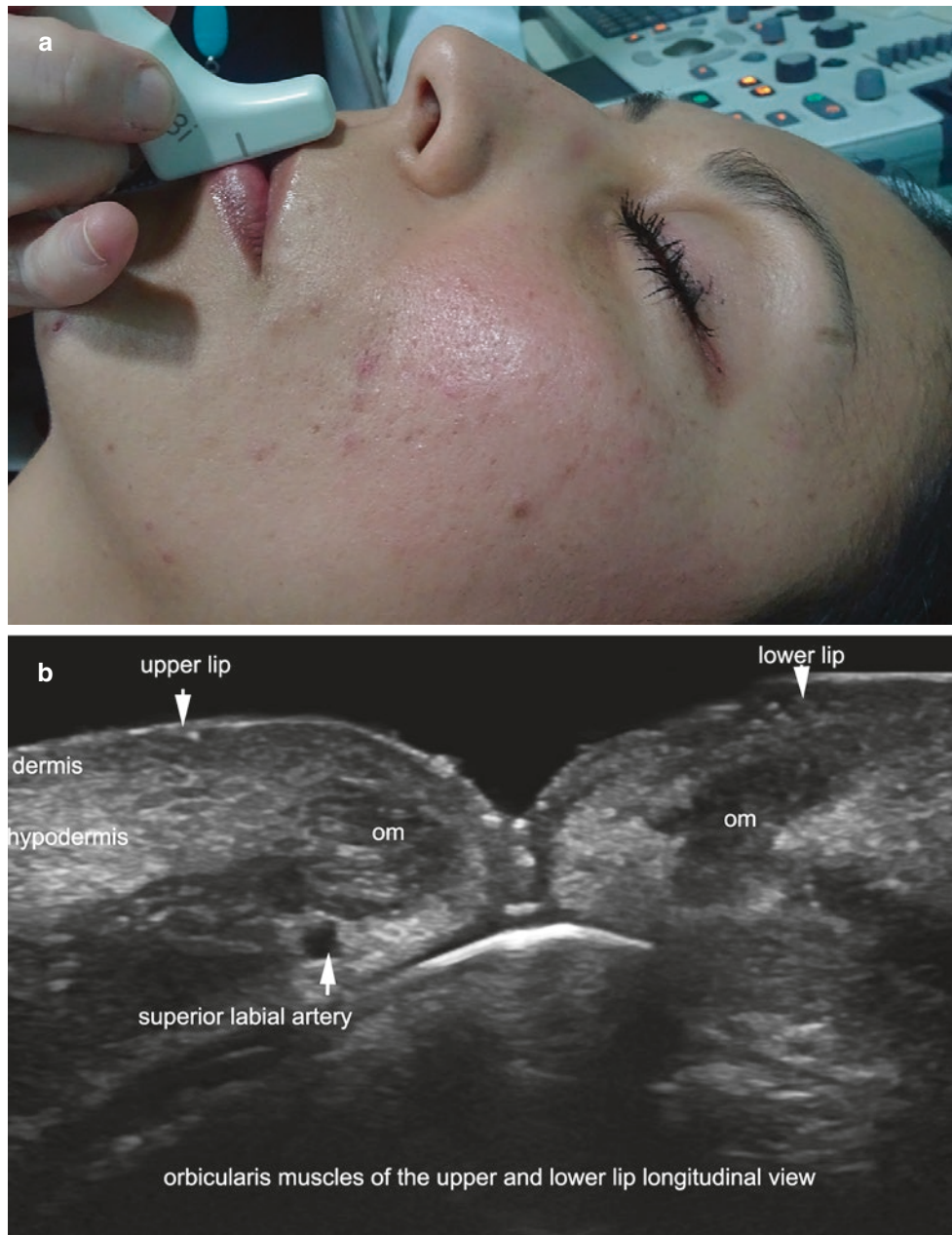


Fig. 6.20 Upper and lower parts of the orbicularis oris muscle. (a) Clinical image shows the location of the probe. (b) Ultrasound (longitudinal axis) shows the hypoechoic bands of the upper and lower parts of the orbicularis muscle at the lips.



Fig. 6.21 Depressor anguli oris muscle. (a) Clinical image shows the location of the probe. (b) Ultrasound (longitudinal panoramic view) shows the hypoechoic structure of the depressor anguli oris muscle. Notice that the muscle (asterisks) is wider in the upper part (left part of the image) close to the modiolus region. (c) Ultrasound (longitudinal

closer view) demonstrates the presence of minor salivary glands (gl) beneath the muscle, which should not be confused with the location of the depressor. (d) Ultrasound (transverse view) shows the wide oval shape of the depressor anguli oris muscle (asterisk) at the proximal region close to the modiolus region. *gl* minor salivary gland, *m* mandible, *t* tooth.

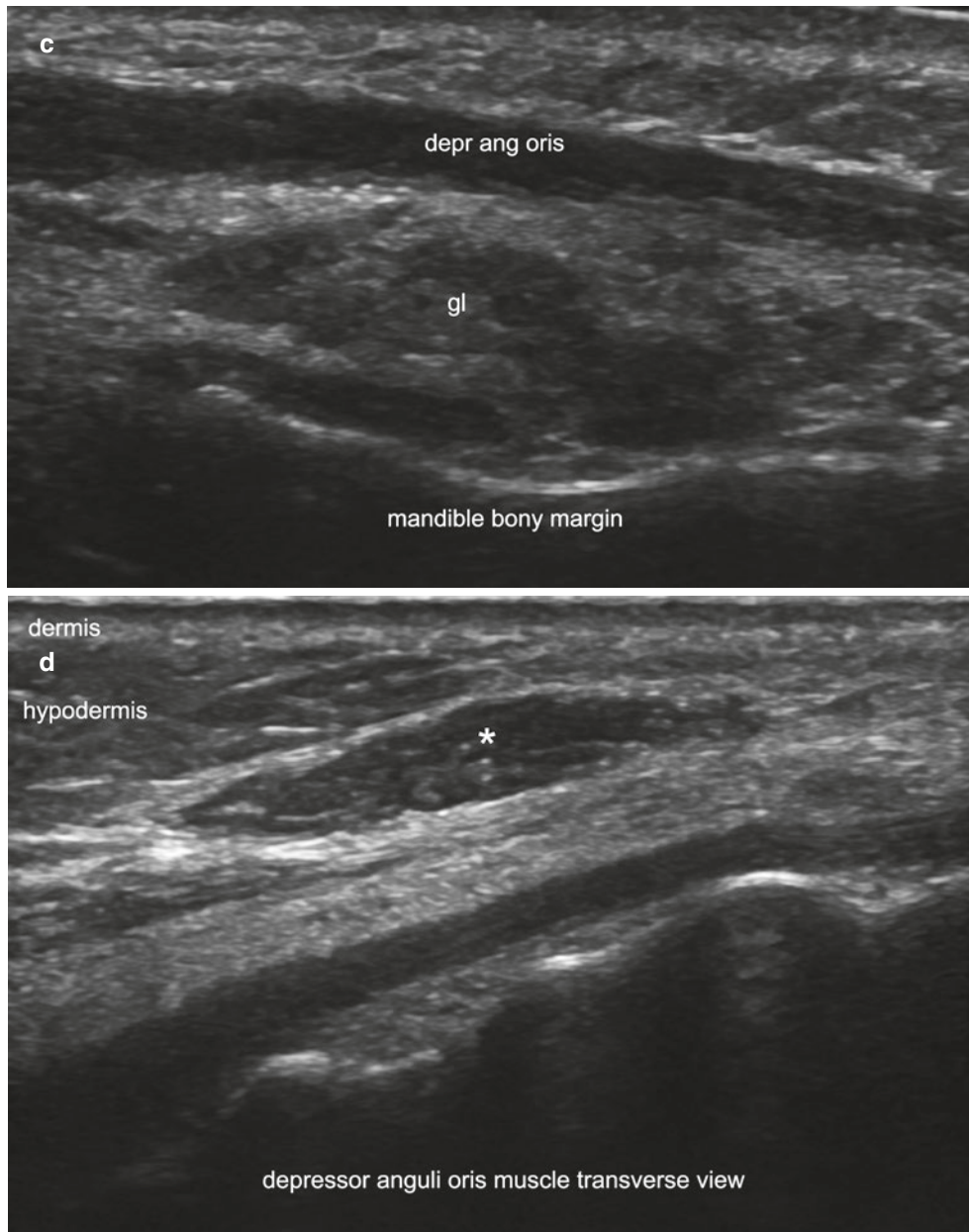


Fig. 6.21 (Continued)

Fig. 6.22 Depressor labii inferioris muscle. **(a)** Clinical image shows the location of the probe. **(b)** Ultrasound (longitudinal oblique view) demonstrates the mostly hyperechoic band of the depressor labii inferioris muscle (depr lab) underneath and medial to the depressor anguli oris muscle (depr angl or). Note that the location of the depressor anguli oris and depressor labii inferioris muscle forms a letter V.



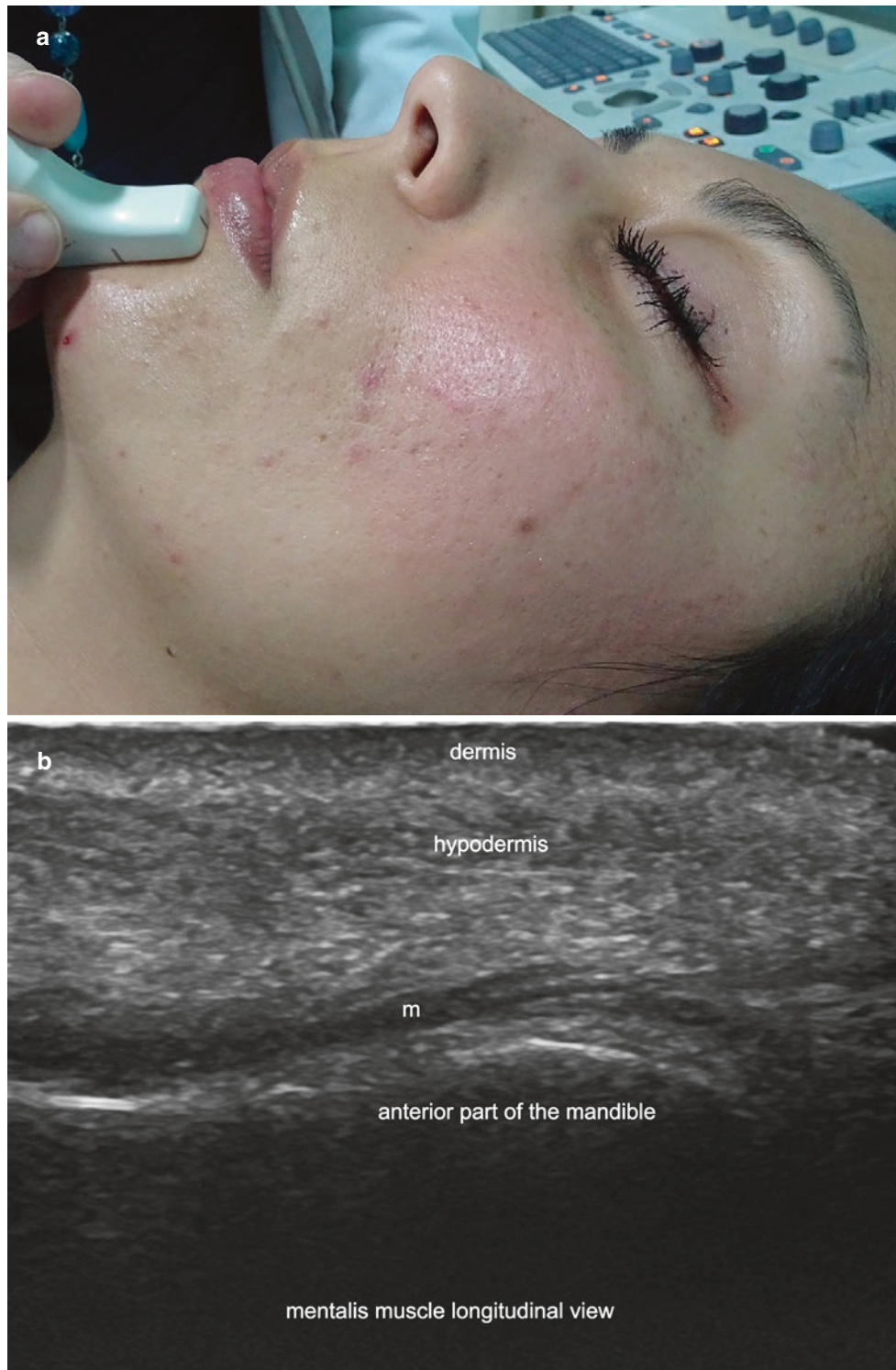


Fig. 6.23 Mentalis muscle. (a) Clinical image shows the location of the probe. (b) Ultrasound (longitudinal oblique view) shows the hypoechoic band of the left band of the mentalis muscle (m) attached to the anterior aspect of the mandible.



Fig. 6.24 Masseter muscle. (a) Clinical image shows the location of the probe. (b) Ultrasound (transverse axis) shows the hypoechoic structure of the masseter muscle, which also contains hyperechoic septa between the muscle fibers.



Fig. 6.25 Buccal fat pad. (a) Clinical image shows the location of the probe. (b) Ultrasound (transverse oblique axis) demonstrates the hypoechoic structure of the buccal fat pad attached to the anterior

aspect of the masseter muscle. Notice the facial artery (fa) running anteriorly to the buccal fat pad.



Fig. 6.26 Facial surface anatomy of the nasal and nasolabial regions. **(a)** Clinical image shows the names of the superficial structures and the level of the location of the probe for detecting the upper and alar nasal cartilages (horizontal lines). **(b)** Ultrasound

(transverse view) demonstrates the hypochoic and homogenous structure of both upper nasal cartilages **(c)**. **(c)** Ultrasound (transverse view) shows the hypochoic structure of the alar nasal cartilages.

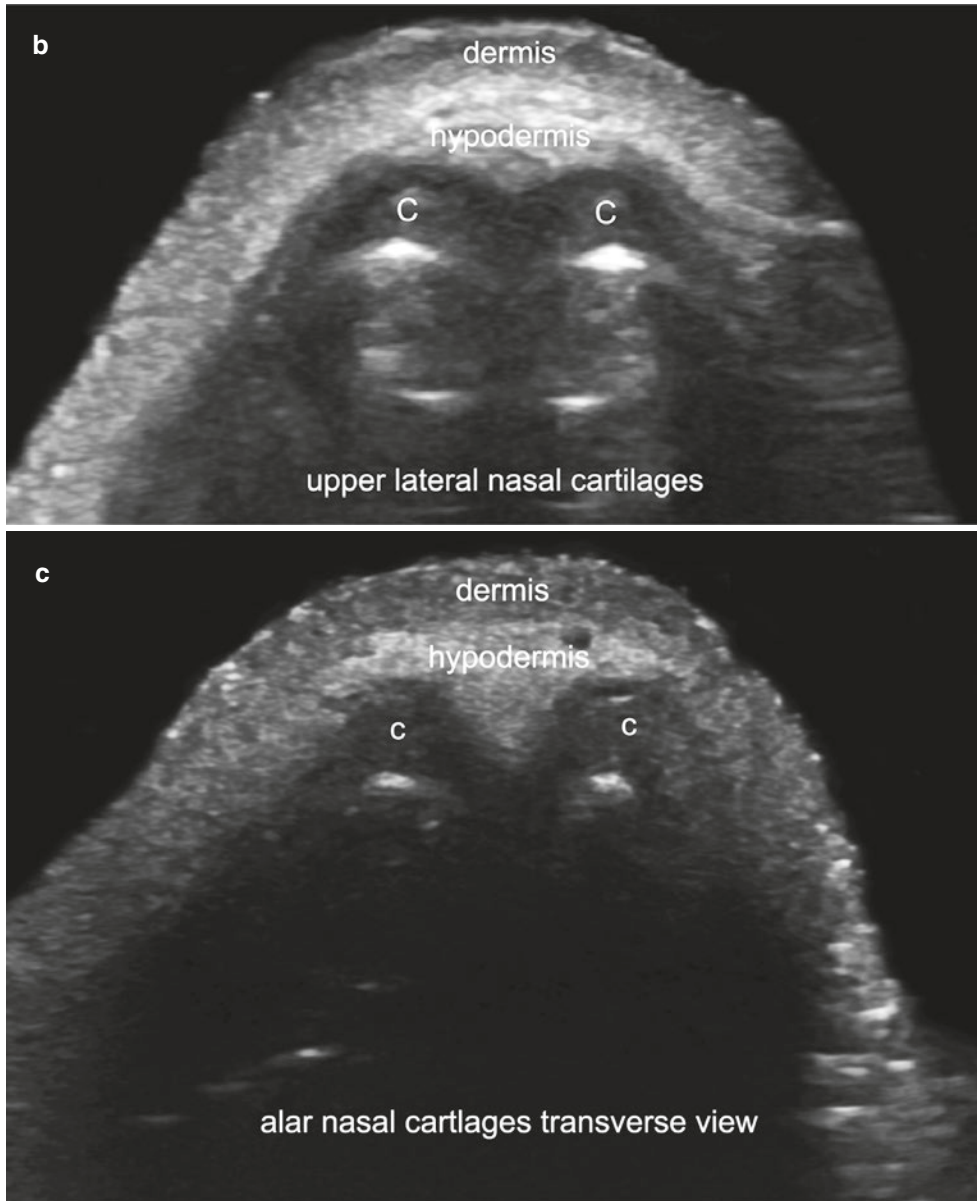


Fig. 6.26 (Continued)



Fig. 6.27 Nasalis muscle. (a) Clinical image shows the location of the probe for detecting the nasalis muscle. (b) Ultrasound (transverse view) demonstrates the hypochoic structure of the left nasalis muscle.



Fig. 6.28 Facial artery. (a) Clinical image shows the location of the probe for tracking the facial artery. It is recommended to start in transverse axis and then turn to the longitudinal axis. (b, c) Color Doppler ultrasound of the facial artery. (b) Transverse view. Notice the location

of the artery (red color) passing anterior to the buccal fat pad. (c) Longitudinal view. The facial artery (in colors) may present a tortuous path; therefore, observation of the artery can require angulation of the probe to follow the axis of the artery.

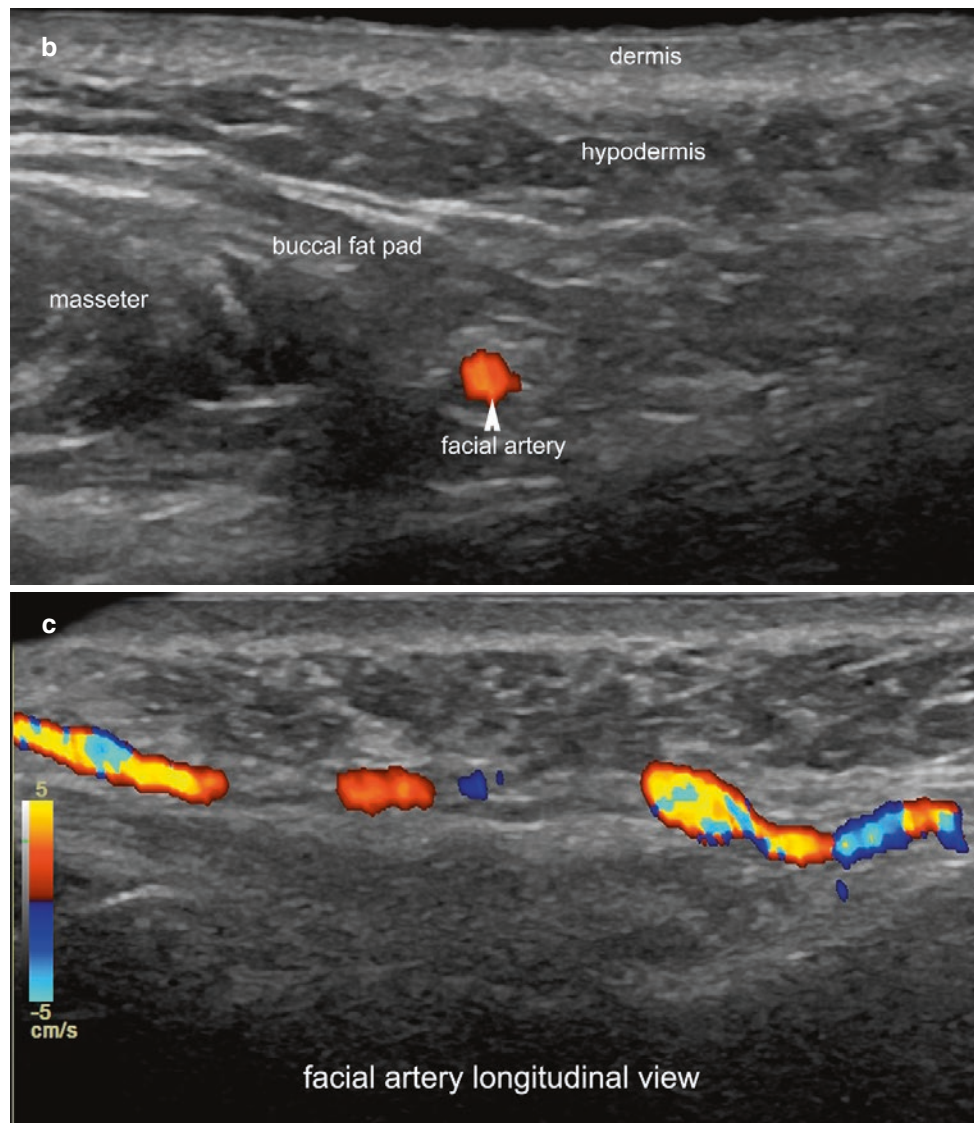


Fig. 6.28 (Continued)



Fig. 6.29 Superior labial and angular arteries. (a) Clinical image shows the recommended positions of the probe for tracking the labial and angular arteries. (b, c) Color Doppler ultrasound. (b), Superior labial artery

(transverse view) at the left border of the upper lip. Notice the location of the labial artery (color) running close to the surface of the teeth (t). (c) Angular artery (longitudinal view) at the paranasal region.

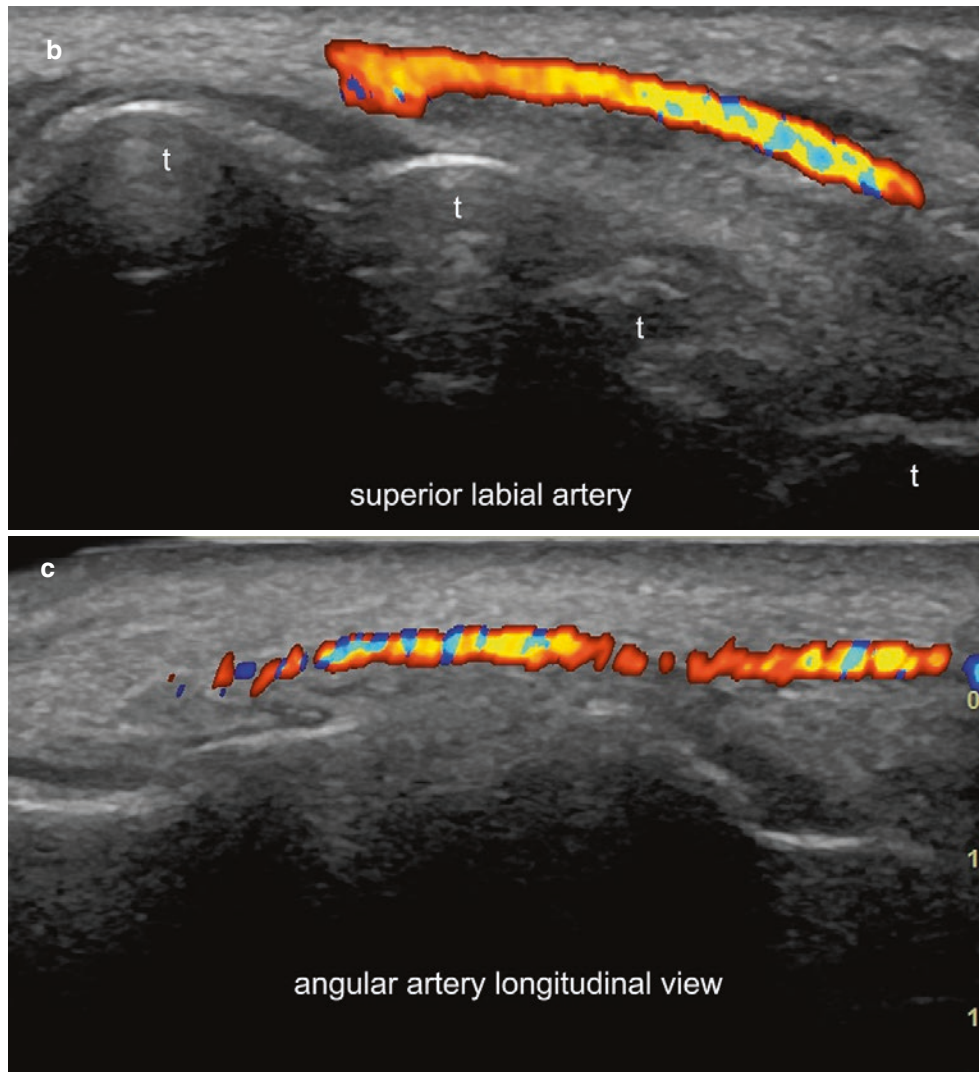


Fig. 6.29 (Continued)

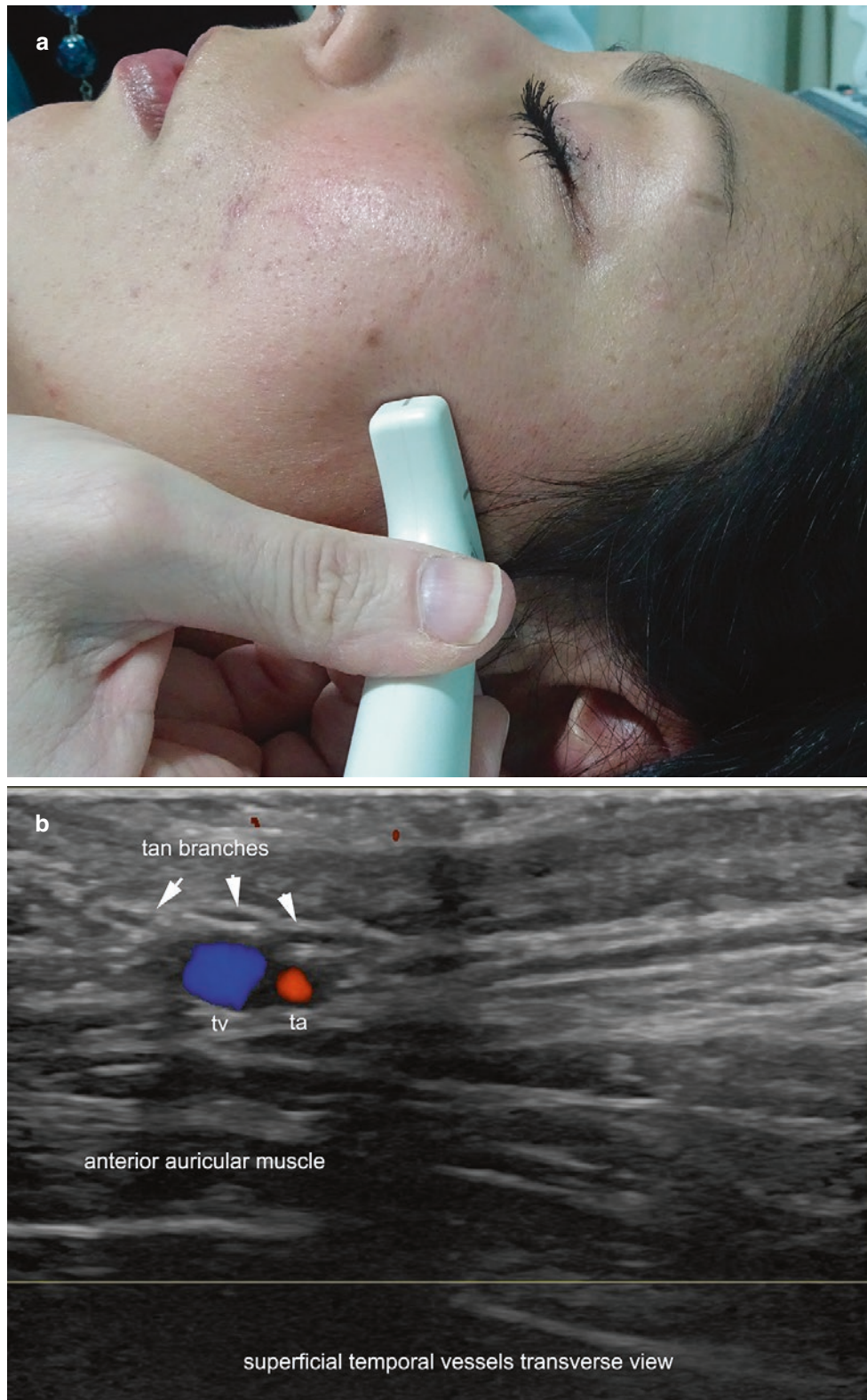


Fig. 6.30 Superficial temporal vessels. (a) Clinical image shows the recommended positions of the probe for tracking the temporal vessels. (b) Color Doppler ultrasound (transverse view) demonstrates the location of the vein (tv) and artery (ta) at the preauricular region. Notice that

three branches of the auriculotemporal nerve (tan) can be seen as oval-shaped, hypoechoic structures (*arrows*) in cross-sectional view, running on top of the superficial temporal vessels.

References

1. Dayan SH. Complications from toxins and fillers in the dermatology clinic: recognition, prevention, and treatment. *Facial Plast Surg Clin North Am.* 2013;21:663–73.
2. Prendergast PM. Anatomy of the face and neck. In: Shiffman MA, Di Giuseppe A, editors. *Cosmetic surgery: art and techniques.* Berlin: Springer; 2013. p. 29–45.
3. Kim HJ, Seo KK, Lee HK, Kim J. *Clinical anatomy of the face for filler and botulinum toxin injection.* Singapore: Springer; 2015.
4. Wortsman X, Wortsman J. Sonographic outcomes of cosmetic procedures. *Am J Roentgenol.* 2011;197:W910–8.
5. Costin BR, Plesec TP, Sakolsatayadorn N, Rubinstein TJ, McBride JM, Perry JD. Anatomy and histology of the frontalis muscle. *Ophthal Plast Reconstr Surg.* 2015;31:66–72.
6. Hwang K, Lee JH, Lim HJ. Anatomy of the corrugator muscle. *J Craniofac Surg.* 2017;28:524–7.
7. Janis JE, Ghavami A, Lemmon JA, Leedy JE, Guyuron B. Anatomy of the corrugator supercillii muscle: part I. Corrugator topography. *Plast Reconstr Surg.* 2007;120:1647–53.
8. Sand JP, Zhu BZ, Desai SC. Surgical anatomy of the eyelids. *Facial Plast Surg Clin North Am.* 2016;24:89–95.
9. Hwang K, Kim HJ, Kim H, Kim DJ, Hwang SW. Origin of the lower orbicularis oculi muscle in relation to the nasojugal groove. *J Craniofac Surg.* 2015;26:1389–93.
10. Pessa JE, Zadoo VP, Garza PA, Adrian EK Jr, Dewitt AI, Garza JR. Double or bifid zygomaticus major muscle: anatomy, incidence, and clinical correlation. *Clin Anat.* 1998;11:310–3.
11. Bo C, Ningbei Y. Reconstruction of upper lip muscle system by anatomy, magnetic resonance imaging, and serial histological sections. *J Craniofac Surg.* 2014;25:48–54.
12. Hur MS, Hu KS, Park JT, Youn KH, Kim HJ. New anatomical insight of the levator labii superioris alaeque nasi and the transverse part of the nasalis. *Surg Radiol Anat.* 2010;32:753–6.
13. Abramo AC, Do Amaral TP, Lessio BP, De Lima GA. Anatomy of forehead, glabellar, nasal and orbital muscles, and their correlation with distinctive patterns of skin lines on the upper third of the face: reviewing concepts. *Aesthet Plast Surg.* 2016;40:962–71.
14. Koerte IK, Schroeder AS, Fietzek UM, Borggraefe I, Kerscher M, Berweck S, et al. Muscle atrophy beyond the clinical effect after a single dose of Onabotulinum toxin A injected in the procerus muscle: a study with magnetic resonance imaging. *Dermatol Surg.* 2013;39(5):761.
15. Bae JH, Choi DY, Lee JG, Seo KK, Tansatit T, Kim HJ. The risorius muscle: anatomic considerations with reference to botulinum neurotoxin injection for masseteric hypertrophy. *Dermatol Surg.* 2014;40:1334–9.
16. Choi YJ, Kim JS, Gil YC, Phetudom T, Kim HJ, Tansatit T, Hu KS. Anatomical considerations regarding the location and boundary of the depressor anguli oris muscle with reference to botulinum toxin injection. *Plast Reconstr Surg.* 2014;134:917–21.
17. Hur MS, Kim HJ, Choi BY, Hu KS, Kim HJ, Lee KS. Morphology of the mentalis muscle and its relationship with the orbicularis oris and incisivus labii inferioris muscles. *J Craniofac Surg.* 2013;24:602–4.
18. Kaya B, Apaydin N, Loukas M, Tubbs RS. The topographic anatomy of the masseteric nerve: A cadaveric study with an emphasis on the effective zone of botulinum toxin A injections in masseter. *J Plast Reconstr Aesthet Surg.* 2014;67:1663–8.
19. Lohn JW, Penn JW, Norton J, Butler PE. The course and variation of the facial artery and vein: implications for facial transplantation and facial surgery. *Ann Plast Surg.* 2011;67:184–8.
20. Cotofana S, Pretterklieber B, Lucius R, Frank K, Haas M, Schenck TL, et al. Distribution pattern of the superior and inferior labial arteries: impact for safe upper and lower lip augmentation procedures. *Plast Reconstr Surg.* 2017;139:1075–82.
21. Tansatit T, Apinuntrum P, Phetudom T. Cadaveric assessment of lip injections: locating the serious threats. *Aesthet Plast Surg.* 2017;41:430–40.
22. Gocmen-Mas N, Edizer M, Keles N, Aksu F, Magden O, Lafci S, et al. Morphometrical aspect on angular branch of facial artery. *J Craniofac Surg.* 2015;26:933–6.
23. Lee WW, Erickson BP, Ko MJ, Liao SD, Neff A. Advanced single-stage eyelid reconstruction: anatomy and techniques. *Dermatol Surg.* 2014;40(Suppl 9):S103–12.
24. Karimnejad K, Walen S. Complications in eyelid surgery. *Facial Plast Surg Clin North Am.* 2016;24:193–203.
25. Alfen NV, Gillhuis HJ, Keijzers JP, Pillen S, Van Dijk JP. Quantitative facial muscle ultrasound: feasibility and reproducibility. *Muscle Nerve.* 2013;48:375–80.
26. Volk GF, Wystub N, Pohlmann M, Finkensieper M, Chalmers HJ, Guntinas-Lichius O. Quantitative ultrasonography of facial muscles. *Muscle Nerve.* 2013;47:878–83.
27. Volk GF, Pohlmann M, Sauer M, Finkensieper M, Guntinas-Lichius O. Quantitative ultrasonography of facial muscles in patients with chronic facial palsy. *Muscle Nerve.* 2014;50:358–65.
28. Volk GF, Pohlmann M, Finkensieper M, Chalmers HJ, Guntinas-Lichius O. 3D-Ultrasonography for evaluation of facial muscles in patients with chronic facial palsy or defective healing: a pilot study. *BMC Ear Nose Throat Disord.* 2014;14:4.
29. Olszewski R, Liu Y, Duprez T, Xu TM, Reychler H. Three-dimensional appearance of the lips muscles with three-dimensional isotropic MRI: in vivo study. *Int J Comput Assist Radiol Surg.* 2009;4:349–52.
30. Tucunduva MJ, Tucunduva-Neto R, Saieg M, Costa AL, de Freitas C. Vascular mapping of the face: B-mode and doppler ultrasonography study. *Med Oral Patol Oral Cir Bucal.* 2016;21:e135–41.
31. Quezada-Gaon N, Wortsman X, Peñaloza O, Carrasco JE. Comparison of clinical marking and ultrasound-guided injection of Botulinum type A toxin into the masseter muscles for treating bruxism and its cosmetic effects. *J Cosmet Dermatol.* 2016;15:238–44.